Development of a New Method for Investigation of the Ash Melting Behavior in the Fluidized Bed Conversion Processes

J.Priscak[1,2*], M.Kuba[1,2], H.Hofbauer[2]

1. BEST – Bioenergy and Sustainable Technologies GmbH, Inffeldgasse 21b, A-8010 Graz, Austria
2. TU Wien, Institute of Chemical, Environmental and Bioscience Engineering (ICEBE), Getreidemarkt 9/166, 1060 Vienna, Austria
*corresponding author, juraj.priscak@best-research.eu

Abstract

The suitability of woody biomass for thermochemical conversion process using fluidized bed technology has already been successfully demonstrated in the last decades. However in lower-rank biomass (e.g. crops and agriculture residues), the ash-forming matter differs from the one in the woody biomass and can cause operational problems such as agglomeration, sintering, fouling, or eventually total defluidization of the fluidized bed. These problems are common for both – combustion and gasifying reactors. Hence the understanding of the ash behavior, as well as creating of a reliable method for the prediction of the ash melting in the fluidized bed is necessary. Several methods such as the ash fusion test, the compression- strength- based test or the controlled fluidization bed agglomeration test can be used to determine the ash melting temperature in the fluidized bed. However none of the test takes into account the influence of the local overheating caused by burning char particles. The following paper focuses on developing a new reliable method to investigate the ash behavior in the fluidized bed.

1. Introduction:

According to the [1], the predicted average annual percent change of the world energy consumption will increase in the next 15 years by 1.5%. In order to meet this increasing demand for energy and also to minimize the air and nature pollution connected to its production, replacing fossil fuels with renewable energy sources is necessary. Already today, renewable energy resources like wind, sun, and water show great potential to compensate a relevant share of fossil fuels as a primary energy source. The most widespread of the renewable energy resources is however biomass, which covers more than 10% of the world primary energy consumption. Especially utilization of waste biomass (agriculture residues, municipal wastes) gained more focus in last years. However, in this type of biomass the ash-forming matter differs from woody biomass and can cause operational problems such as sintering, agglomeration or eventually total defluidization of the fluidized bed. These problems are common for both – combustion and gasification reactors. Hence, the understanding of the ash melting behavior, as well as the creating a reliable method for predicting the operational problems in fluidized bed systems is necessary. There are number of techniques to predict ash behavior during thermochemical conversion processes, focused mostly on bed agglomeration. The ASTM ash fusion test is a standard method based on the visual indication of the softening and melting behavior of the test sample [2]. Although it has been repeatedly reported as a poor method for determination of ash related problems

[3],[4],[5] it is still widely used due to its simplicity. Skrifvars et al. proposed a method for the prediction of the biomass sintering, based on the compression strength tests and the thermodynamic equilibrium calculations [4]. The method highlights the importance of the bed sintering due to partially ash melting and its contribution to the bed agglomeration and to the deposit formation. However, both methods suffer from exclusion of the interaction between ash and bed material. Öhman and Nordin developed a more reliable method for prediction of bed agglomeration tendencies in fluidized bed combustion (FBC) boilers [6]. According to the method, the fuel is first combusted in oxidizing atmosphere in a fluidized bed (FB) reactor until sufficient amount of ash is produced. Afterwards the fuel feeding is stopped and the bed temperature is linearly increased by applying external heat to the primary air and to the reactors walls. The initial agglomeration temperature is determined by a sudden temperature and pressure drop in the bed. However, since the local overheating of the burning char particles is absent in the test, it remains unclear, how well the results reproduce the bed agglomeration in a full-scale FB reactor [3]. Moreover, the progressive accumulation of ash in the bed is not accounted for either, which can be problematic in the case of fuels like e.g. lignin or rice husk, in which coherent ash particles are formed during steady state combustion and can cause serious operational problems. As the experiments with lignin showed, the stability and morphology of the ash particles depends not only on the combustion temperature, but on the combustion regime as well, and therefore above-mentioned methods may not simulate the real behavior of the ash during combustion of such fuels. For example, rapid combustion of lignin in the fluidized bed at temperatures above 700°C leads to an extensive formation of such particles, which accumulates at the top of the bed. Such combustion regime is present in the fluidized bed reactor, where the fuel particle is introduced into the reactor already at elevated temperature and rapidly heated. On the other hand, if the ash is being produced with a technique, which involves a preheating step at lower temperature followed by a slow increase in temperature (without char burnout), the result is a loose ash, which will be in FB carried out as a fly ash. Therefore in order to fully investigate the biomass ash melting behavior during combustion in the fluidized bed reactor at different bed temperatures, it is necessary to develop a method, which includes burning of the char particle as well. Such method has been proposed and tested in the lab-scale reactor with wheat straw and wheat straw lignin.

2. Concept and methodology:

2.1. Fuel characterization

Wheat straw and wheat straw lignin have been pelletized prior to the experiments in the FB reactor and the furnace oven. **Fehler! Verweisquelle konnte nicht gefunden werden.** shows fuels properties, obtained by corresponding norm methods (water content by DIN 51718; ash content by EN ISO 18022; volatiles by EN ISO 18023; lower heating value by DIN 51900 T2; initial deformation temperature (IDT) by CEN/TS 15370-1).

	Wheat straw	Lignin
Moisture (wt.%)	7.2	6.06
Ash content ($wt.\%_{d.b}$)	7.5	15.47
Volatiles ($wt.\%_{d.b}$)	74.7	64.88
LHV (kJ/kg)	16860	18779
IDT (°C)	830	1430

Tab. 1: Important combustion parameters of wheat straw and lignin

Furthermore, a XRF analysis of the fuel ashes was performed by Test Laboratory for Combustion Systems at TU Vienna with the Axios Advanced Analyser from company Panalytical. The mass of individual elements were measured and afterwards recalculated to oxides (Tab. 2).

Oxide	Wheat straw	Lignin
Fe_2O_3	1.81	0.71
CaO	4.43	3.76
K_2O	12.26	3.08
P_2O_5	2.71	1.23
SiO_2	60.88	84.46
Al_2O_3	1.52	2.62
MgO	4.32	0.35
Na_2O	2.56	1.48

Tab. 2: Ash composition of fuels (wt.%)

Low alkali content of lignin (compared to wheat straw) origins in a leaching step of the process, where lignin is extracted as a byproduct. **Fehler! Verweisquelle konnte nicht gefunden werden.** shows results from an elemental analysis, performed at Microanalytical Laboratory at Institute for Physical Chemistry at TU Vienna. Total sulfur and chlorine content was determined by the norm method EN ISO 16994.

Element	Wheat straw	Lignin
Carbon	45.09	51.67
Hydrogen	5.75	3.49
Nitrogen	0.55	1.43
Sulfur	0.12	0.123
Chlorine	0.09	0.025

Tab. 3: Elemental analysis of wheat straw and lignin (wt.%)

2.2. Experiments in the lab-scale reactor

Experiments with both fuels have been performed in the lab-scale reactor with an electric power of 1.5kW. **Fehler! Verweisquelle konnte nicht gefunden werden.** shows a schematic of the reactor, including the positioning of the temperature and pressure measurement. The reactor has an inner diameter of 5.3 cm and a bed height of 10 cm and is made of stainless steel. Before the air is distributed into the reactor through a perforated plate, it is heated with a temperature regulator and with a cylindrical electrical furnace with the power of 750 W. The fluidized bed section is heated up using a uniform cylindrical electrical furnace with the same power output. Air volume flow of 20 Nl/min has been used, what corresponds to a U/U_{mf} ratio of approx. 20. In total, five K-type thermocouples monitor the temperatures of the fluidized bed, the freeboard, the fuel bunker, the flange sealing as well as the temperatures of the wall of preheater and reactor heater. The pressure sensor is situated before the distribution plate, so the pressure drop across the bed can be calculated from the difference between atmospheric and measured pressure. Feedstock pellets are transported from the feedstock bunker into the reactor with a screw conveyor. The used method consists of two parts. In the first part the ash is produced in the reactor through the fuel combustion. Approximately 300 g/h of the fuel have been continuously supplied into the reactor by the screw conveyor. Quartz sand (300 g) with a particle diameter between 400-500 µm has been used as a bed material. The bed material has been fluidized with 20 Nl/min of air and temperature held at 650 °C by adjusting the external heaters power. After approx. 1 hour of the ashing phase, the bed temperature is increased in steps of 50 °C (part 2) by external electrical heater (while maintaining constant fuel supply of 300

g/h) until reaching the bed temperature of 950-1000 °C.

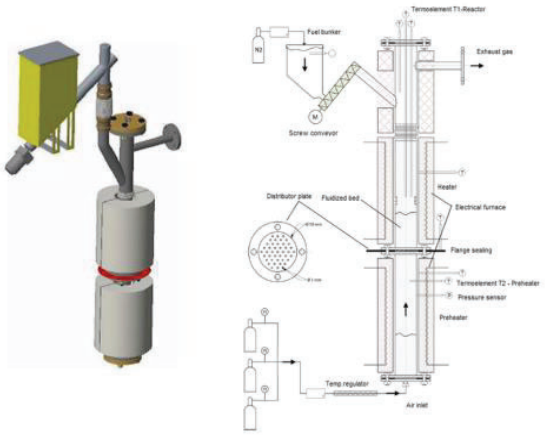

Fig. 1: Scheme of the lab-scale fluidized bed reactor [7]

2.3. Experiments in the furnace oven

In order to further investigate the formation of coherent ash particles during lignin combustion (Chapter 3.1), additional experiments in the furnace oven have been performed. During the experiments, lignin pellets have been burned in an electrical furnace oven in two regimes. Air has been used as an oxidizing agent in both cases. The first regime (combustion at low heating rate) included preheating phase, where the sample was at first continuously heated to 250 °C in 30 min. The temperature in the furnace oven has been then kept constant at 250 °C for 120 min. Afterwards the sample was heated up to 600 °C (Sample 1), 700 °C (Sample 3) and 800 °C (Sample 5) and burnt at constant temperature for another 210 min. During the second regime (without preheating; combustion at high heating rate) the sample was inserted into the furnace oven already at combustion temperature (600 °C, 700 °C and 800 °C for Sample 2, 4, 6 accord.) for 210 min. Afterwards the samples have been cooled down to a room temperature and further examined by XRF and XRD analysis.

2.4. Chemical equilibrium calculations

Thermochemical equilibrium calculations have been performed using the software Factsage 7.3 in the Equilib module, which employs the Gibbs energy minimization algorithm and thermochemical functions. The fuel ash composition (Tab. 2) has been used as a reactant stream. The amount of air, necessary for total combustion, has been subsequently calculated in Factsage. FactPS, FToxid and FTsalt have been chosen as databases. Solutions FToxide-SLAGA and FTsalt-SALTB have been used in calculations for both fuels.

3. Results and discussion

3.1. Behavior of wheat straw and lignin in fluidized bed combustion

Fehler! Verweisquelle konnte nicht gefunden werden. shows the results of the experiment with wheat straw. As can be seen from temperature and pressure measurement, the bed collapses approx. at 03:30 (overall operating time, including the initial heating of the reactor).

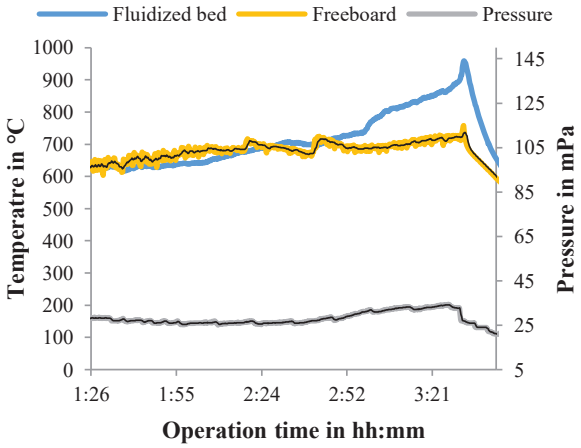

Fig. 2: Temperature and pressure profile of the wheat straw combustion in the FB reactor

This time corresponds to the bed temperature of 865 °C and the ash content of 20 wt.%$_{d.b.}$ (with no regards on the ash that has been carried out from the reactor). The melting temperature of wheat straw based on thermodynamic equilibrium calculations (Fig. 6) is 750 °C, what exceeds measured value by 100 °C.

Although the melting phase occurs already at 650 °C, at least 15-30 wt.% of the ash needs to be molten in order for an ash particle to be sticky [8]–[10]. After the reactor was cooled down and opened, agglomerates were found in the bed (Fig. 3).

Fig. 3: Bed agglomerates from combustion of wheat straw in the FB reactor

The experiment with lignin started with the ashing phase (approx. 1 hour) as well. The amount of ash in the reactor after 1 hour corresponds to approx. 7 wt.%$_{db}$. The temperature of the bed has been afterwards continuously increased with an electrical heater. At approx. 4:22 pressure fluctuations occurred and the fuel supply was turned off.

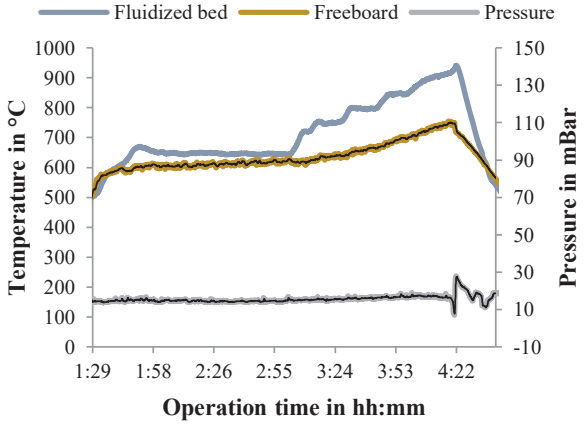

Fig. 4 : Temperature and pressure profile of lignin combustion in the FB reactor

As have been found later, the bed collapse was caused by coherent ash residues (Fig. 5), which were accumulated at the top of the bed.

Fig. 5: Coherent ash particles from combustion of lignin in the FB reactor

No bed agglomeration occurred, what has been also supported by equilibrium calculations. As can be seen at **Fehler! Verweisquelle konnte nicht gefunden werden.**, the amount of molten ash does not exceed 30 wt.%. However partially molten ash is responsible for the mechanical stability of the ash particles, which increases above 850 °C. Therefore if the method is used, where ash is prepared at temperature under 700 °C and then continuously heated up, such problematic behavior of the fuel ash may not be detected.

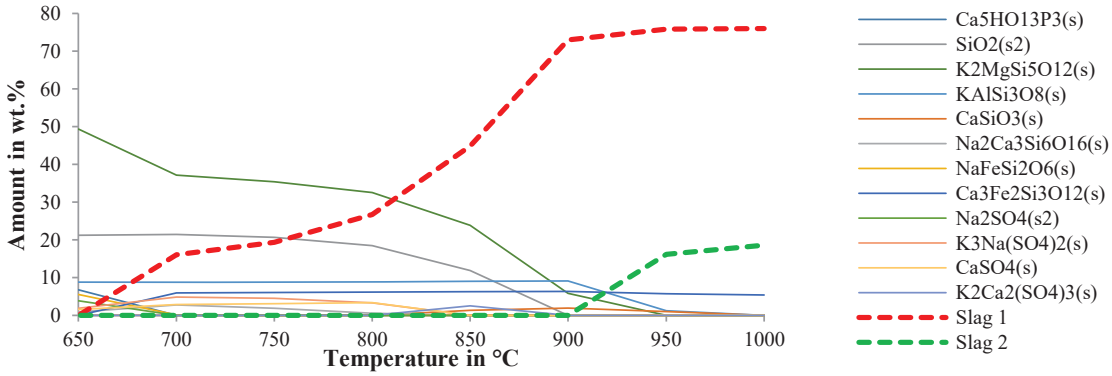

Fig. 6: Equilibrium calculations based on wheat straw ash composition

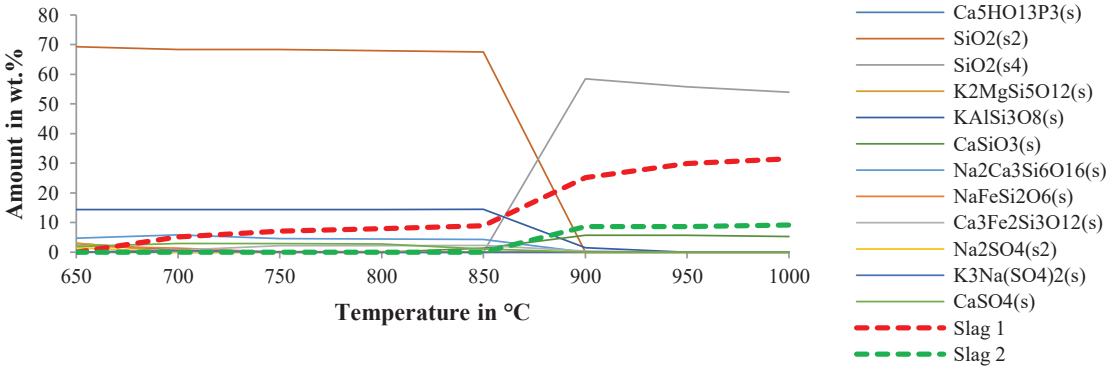

Fig. 7: Equilibrium calculations based on lignin ash composition

3.2. Behavior of lignin ash at different combustion regimes

Experiments in the furnace oven at different combustion temperatures show strong dependence between the formation of dimensionally stable ash particles and the combustion regime. Combustion of particles without preheating, where the sample is introduced into the furnace oven at typical operating temperatures (Fig. 8, left column), leads to a formation of dimensionally stable or coherent ash particles. On the other hand, if the samples are first dried at 250°C and then continuously heated up to typical operating temperatures (Fig. 8, right column), the result will be a formation of more fragile ash particles.

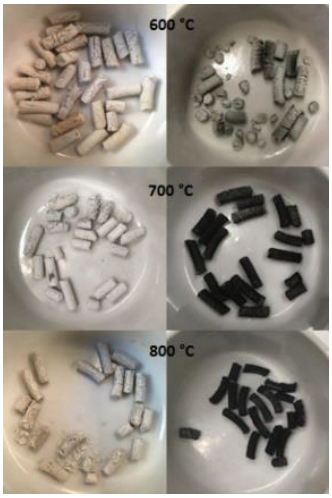

Fig. 8: Samples 1-6; Combustion with (left) and without (right) preheating step

Samples from the experiments in the furnace oven were further analyzed with an X-ray diffraction (Fig. 9). In all 6 cases, majority of the sample is present in the amorphous phase. Crystalline phase is composed mainly of cristobalite, quartz and arcanite. Up to 700 °C, quartz is the dominant silica polymorph in the crystalline phase. Above 700 °C,

crystallization of cristobalite (with peak at 21-22 °2Theta) from amorphous phase occurs.

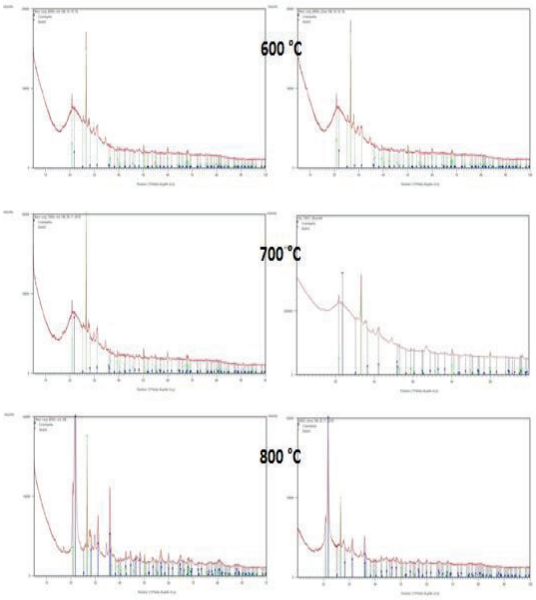

Fig. 9: XRD Analyis of the samples 1-6; Combustion with (left) and without (right) preheating step

From comparison of XRD patterns is apparent, that crystallization of cristobalite and quartz from amorphous phase dependent on combustion temperature and is practically independent of combustion regime. Similar observations have been made by combustion of rice hulls [11]–[14], [15]. Venezia et al. [11] examined effects of alkali ions on these transitions and concluded, that both Na^+ and K^+ ions destabilize the amorphous silica and support crystallization of silica polymorphs like quartz, cristobalite and tridymite. Moreover, Nakata et al. [15] found , that potassium contained in the rice hull ash accelerate the crystallization of amorphous SiO_2 to cristobalite. Hence, more extensive crystallization of cristobalite is connected to the potassium content in the ash and its availability for the chemical reaction. As can be seen in **Fehler! Verweisquelle konnte nicht gefunden werden.**, the potassium content in the examined samples 1-6 is comparable. However, different heating regimes lead to variant reaction pathways of alkali ions during combustion and gasification.

Sample	1	2	3	4	5	6
Temperature	600 °C	600 °C	700 °C	700 °C	800 °C	800 °C
Heating rate	Low	High	Low	High	Low	High
Fe_2O_3	0.90	0.82	0.77	0.91	0.87	0.95
CaO	6.87	7.14	6.41	6.70	6.88	7.23
K_2O	3.87	3.54	3.36	3.95	3.81	4.34
P_2O_5	2.88	3.01	2.85	2.85	2.84	2.86
SiO_2	79.2	80.0	79.4	80.2	79.5	76.4
Al_2O_3	1.26	2.15	2.86	1.85	1.41	2.81
MgO	1.06	0.93	0.86	1.03	1.04	1.17
Na_2O	1.12	0.65	0.95	0.85	0.91	2.44
SO_3	2.22	1.36	2.09	1.14	2.23	1.00

Tab. 4: XRF Analysis of Sample 1-6

Sulfur, which concentrations vary in the different samples, may play an important role in these pathways. Sulfur and potassium behavior during the combustion of biomass were investigated by Knudsen et al.[16]. According to the authors, 40-50 % of total sulfur is released into the gas phase in the interval between 500-800 °C. On the contrary, only a little (<10%) or none potassium is released below 700 °C.

In their other paper [17] Knudsen et al. have observed, that sulfur is upon heating not released directly into the gas phase, but rather transformed into another form of solid sulfur, such as alkali sulfate [18]. Consequently potassium sulfates will be formed at lower heating rates and preserved in the crystal form during char burn-off, since the melting point of potassium sulfate reaches ~1300 °C. However, upon rapid heating (gasification, combustion) potassium and sulfur are released into the gas phase simultaneously, enabling the reaction between potassium and silica which leads to a formation of alkali silicates with low melting point. Without reaction partner from a solid state, sulfur will be released into gas phase, decreasing its content in e.g. Sample 4 (700 °C, high HR), in comparison to Sample 3 (700 °C, low HR). Equilibrium calculations in Factsage 7.3 also predicted formation of K_2SO_4(s2) in both cases. In the case of sample 2, 4 and 6 considerably lower amounts of K_2SO_4(s2) leads to a formation of $K_2Si_4O_9$(s) which is further transformed into liquid Slag 1 (Fig. 11). On the other hand, if enough sulfur is available for capturing potassium in the form of K_2SO_4(s2), potassium silicates will not form and consequently liquid slag (Slag 1 and Slag 2) will form earliest at temperatures above 900 °C (Fig. 10).

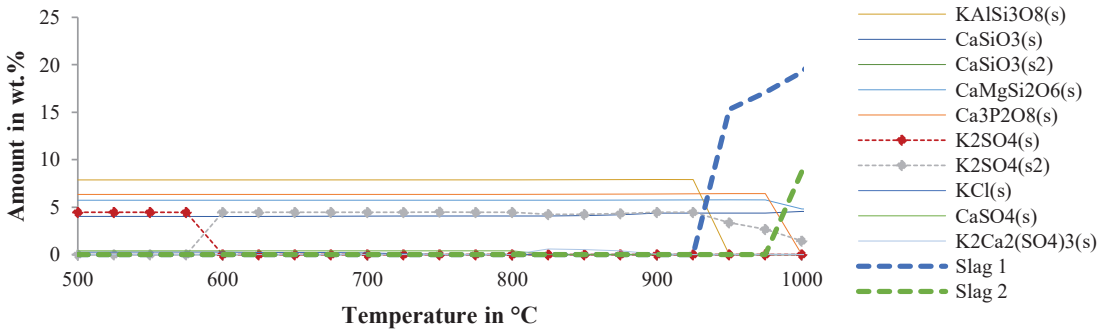

Fig. 10: Equilibrium calculations based on ash composition of Sample 3

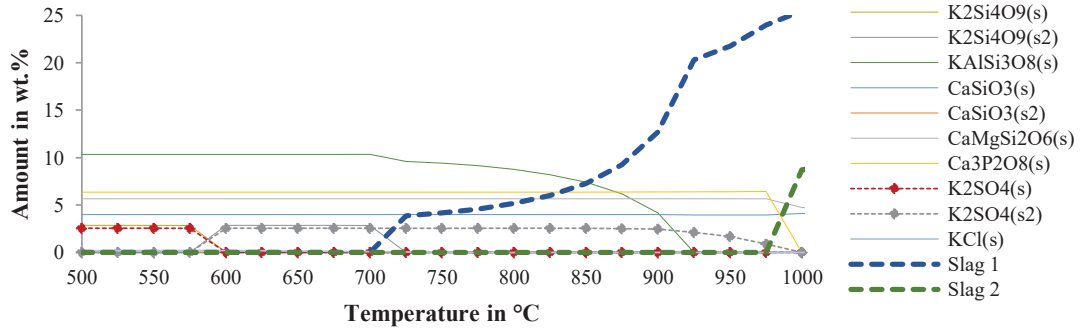

Fig. 11: Equilibrium calculations based on ash composition of Sample 4

3.3. Comparison of ash behavior methodologies

*bed collapse caused by accumulation of ash residues

Tab. 5 shows comparison of the ash melting temperatures acquired by the standard ASTM fusion test, equilibrium calculations in Factsage and the experiments in the FB reactor.

	Wheat Straw	Lignin
ASTM	830 °C	1430 °C
Factsage	800 °C	900 °C
FB reactor	865 °C	900 °C*

*bed collapse caused by accumulation of ash residues

Tab. 5: Comparison of ash melting temperatures from the ASTM test, equilibrium calculations and the experiment in FB reactor

In the case of wheat straw, the temperature determined by the ASTM test is comparable with agglomeration temperature from the experiments in the FB reactor, at which bed particles adhere together due to molten ash (so called "melt-induced" agglomeration). However, as already established by several authors, the ASTM fusion test fails to predict the agglomeration temperature in most cases, since the interactions between ash particles and bed material are excluded from the test. These interactions may lead to a formation of a uniform coating on the bed material surface, which at elevated temperatures may initiate agglomeration ("coating-induced agglomeration"). On the other hand, the method proposed by Öhman and Nordin [6] is suitable for determination of both agglomeration types. However it may not be able to detect other problematic ash behavior – formation and accumulation of the coherent ash particles in the fluidized bed. As have been showed in Chapter 3.2, the formation of such particles is due to reaction pathways enhanced above certain temperature. Therefore it is necessary, in order to detect such problematic ash behavior, to include char particle burning in the used method. Such method has been proposed and tested with wheat straw and wheat straw lignin. The developed method is capable to determine the bed agglomeration temperature ("melt-induced agglomeration"), as well as formation and accumulation of coherent ash particles. Suitability of the proposed method for determination of "coating-induced" agglomeration is however still subject for further investigation.

4. Conclusion and Outlook

A new method for investigation of the ash behavior in the fluidized bed combustion, which besides ash-bed material interactions also accounts for the influence of local overheating caused by burning char particles has been developed and tested. In the case of wheat straw, agglomeration temperature of 865 °C has been determined, what is in good agreement with the results of chemical equilibrium calculations (800 °C). The developed method has been also able to detect another problematic ash behavior – formation of coherent ash particles during combustion of wheat straw lignin. These ash particles were accumulated at the top of the fluidized bed and caused bed collapse. Formation of the particles was caused by molten phase, what was predicted by equilibrium calculations as well.

5. Acknowledgements

This study was carried out within the Bioenergy2020+ GmbH project C200410. Bioenergy2020+ GmbH is funded within the Austrian COMET program, which is managed by the Austrian Research Promotion Agency (FFG) and promoted by the federal government of Austria as well as the federal states of Burgenland, Niederösterreich, and Steiermark. We are grateful for the support of our project partners HGA Senden (Stadtwerke Ulm), Bertsch Energy, Quarzwerke and Institute of Chemical, Environmental and Bioscience Engineering (ICEBE).

6. References

[1] S. C. Davis, W. Hay, und J. Pierce, Biomass in the energy industry: An introduction, London (GB): BP plc, 2014.

[2] D. ASTM, 87: Standard Test Method for Fusibility of Coal and Coke Ash, 1985 Annual Book of Standards, Bd. 5, 1857.

[3] F. Scala, Particle agglomeration during fluidized bed combustion: Mechanisms, early detection and possible countermeasures, Fuel Processing Technology, Bd. 171, S. 31–38, März 2018.

[4] B.-J. Skrifvars, R. Backman, und M. Hupa, Characterization of the sintering tendency of ten biomass ashes in FBC conditions by a laboratory test and by phase equilibrium calculations, Fuel Processing Technology, Bd. 56, Nr. 1, S. 55–67, Juli 1998.

[5] B.-J. Skrifvars, M. Öhman, A. Nordin, und M. Hupa, Predicting Bed Agglomeration Tendencies for Biomass Fuels Fired in FBC Boilers: A Comparison of Three Different Prediction Methods, Energy Fuels, Bd. 13, Nr. 2, S. 359–363, März 1999.

[6] M. Öhman und A. Nordin, A New Method for Quantification of Fluidized Bed Agglomeration Tendencies: A Sensitivity Analysis, Energy Fuels, Bd. 12, Nr. 1, S. 90–94, Jan. 1998.

[7] D. Eßletzbichler, Auslegung, Aufbau und Inbetriebnahme einer Wirbelschichtapparatur im Labormaßstab für thermische Umwandlungsprozesse von Biomasse, S. 161, 2017.

[8] N. Evic, T. Brunner, und I. Obernberger, „Prediction of biomass ash melting behavior “, S. 8, 2012.

[9] M. Zevenhoven-Onderwater, J.-P. Blomquist, B.-J. Skrifvars, R. Backman, und M. Hupa, The prediction of behaviour of ashes from five different solid fuels in fluidised bed combustion, Fuel, Bd. 79, Nr. 11, S. 1353–1361, Sep. 2000.

[10] D. Lundmark, C. Mueller, B.-J. Skrifvars, und M. Hupa, „Computational fluid dynamic model of combustion and ash deposition in a biomass-cofired bubbling fluidized bed boiler, Clean Air: International Journal on Energy for a Clean Environment, Bd. 8, Nr. 2, S. 155–169, 2007.

[11] A. M. Venezia, V. La Parola, A. Longo, und A. Martorana, Effect of Alkali Ions on the Amorphous to Crystalline Phase Transition of Silica, Journal of Solid State Chemistry, Bd. 161, Nr. 2, S. 373–378, Nov. 2001.

[12] Y. Shinohara und N. Kohyama, Quantitative Analysis of Tridymite and Cristobalite Crystallized in Rice Husk Ash by Heating, Ind Health, Bd. 42, Nr. 2, S. 277–285, 2004.

[13] T. Okutani, Utilization of silica in rice hulls as raw materials for silicon semiconductors, Journal of Metals, Materials and Minerals, Bd. 19, Nr. 2, Apr. 2017.

[14] S. Chandrasekhar, K. G. Satyanarayana, P. N. Pramada, P. Raghavan, und T. N. Gupta, Review Processing, properties and applications of reactive silica from rice husk—an overview, Journal of Materials Science, Bd. 38, Nr. 15, S. 3159–3168, Aug. 2003.

[15] Y. Nakata, M. Suzuki, T. Okutani, M. Kikuchi, und T. Akiyama, Preparation and Properties of SiO2 from Rice Hulls, J. Ceram. Soc. Japan, Bd. 97, Nr. 1128, S. 842–849, Aug. 1989.

[16] J. N. Knudsen, P. A. Jensen, und K. Dam-Johansen, Transformation and Release to the Gas Phase of Cl, K, and S during Combustion of Annual Biomass, Energy Fuels, Bd. 18, Nr. 5, S. 1385–1399, Sep. 2004.

[17] J. N. Knudsen, P. A. Jensen, W. Lin, F. J. Frandsen, und K. Dam-Johansen, Sulfur Transformations during Thermal Conversion of Herbaceous Biomass, Energy Fuels, Bd. 18, Nr. 3, S. 810–819, Mai 2004.

[18] P. Glarborg und P. Marshall, „Mechanism and modeling of the formation of gaseous alkali sulfates“, Combustion and Flame, Bd. 141, Nr. 1, S. 22–39, Apr. 2005.